

Covalently Linked Ruthenium(II)–Manganese(II) Complexes: Distance Dependence of Quenching and Electron Transfer

Katja E. Berg,^[a] Anh Tran,^[a] Mary Katherine Raymond,^[b] Malin Abrahamsson,^[b] Juliusz Wolny,^[c] Sophie Redon,^[a] Mikael Andersson,^[b] Licheng Sun,^[a] Stenbjörn Styring,^[d] Leif Hammarström,^{*[b]} Hans Toftlund,^{*[c]} and Björn Akermark^{*[a]}

Keywords: Ruthenium / Manganese / N ligands / Electron transfer

Continuing our development of artificial models for photosystem II in green plants, a series of compounds have been prepared in which a $\text{Ru}(\text{bpy})_3^{2+}$ photosensitizer is covalently linked to a manganese(II) electron donor. In addition to a tris-picolylamine ligand, two other manganese ligands, dipicolylamine and aminodiacetic acid, have been introduced in order to study ligands that are appropriate for the construction of manganese dimers with open coordination sites for the binding of water. Coordination equilibria of the manganese ions

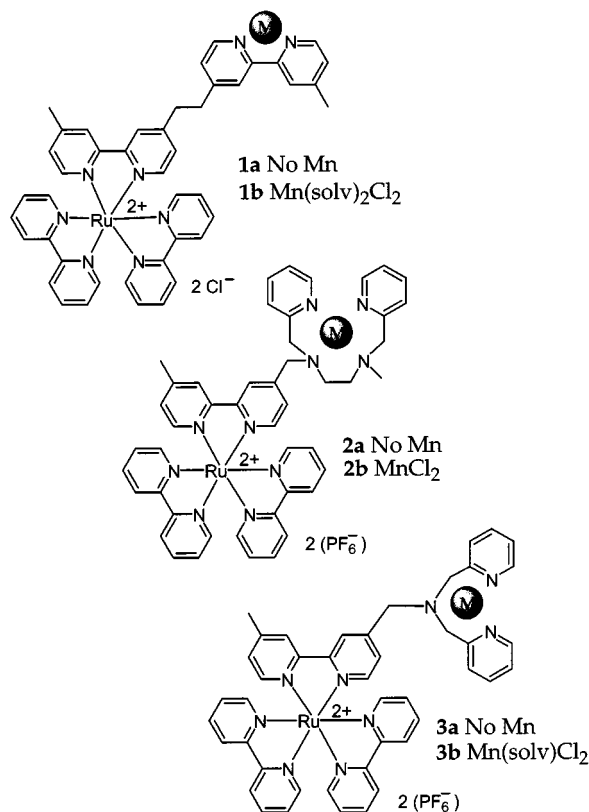
were monitored by EPR. The interactions between the ruthenium and manganese moieties were probed by flash photolysis, cyclic voltammetry and steady-state and time-resolved emission measurements. The quenching of the Ru^{II} excited state by Mn^{II} was found to be rapid in complexes with short Ru–Mn distances. Nevertheless, each Ru^{II} species could be photo-oxidized by bimolecular quenching with methylviologen, and the subsequent electron transfer from Mn^{II} to Ru^{III} could be monitored.

Introduction

Considerable efforts have been made to create biomimetic systems for natural photosynthesis.^[1] The search for alternative renewable energy sources often underlies this research, and there is a need to understand, at a fundamental level, how nature converts solar energy into chemical forms that can be stored. An important subject involves the structure and function of the manganese cluster in the oxygen-evolving complex (OEC) in photosystem II (PS II).^[2–3]

To date, biomimetic systems have focused either on new polynuclear manganese model complexes, or on supramolecular assemblies based on porphyrins and transition metal complexes.^[4–5] Our aim has been to use the principles of the natural PS II to construct supramolecular complexes in which a photosensitizer is covalently linked to one or several manganese ions. Ultimately, the idea in this project is to imitate Nature by photochemically oxidizing water to form oxygen, and to use the electrons released in this process to generate fuels, for example, H_2 .

As an artificial replacement for the chlorophyll photosensitizer in PS II, we have used Ru^{II} trisbipyridyl complexes because they have favorable photochemical properties and are stable and relatively easy to synthesize. With complex **1b**, it was demonstrated that upon photo-oxidation of the Ru^{II} complex by an external acceptor, electron transfer oc-



curred from Mn^{II} to Ru^{III} .^[6] However, the rate of electron transfer in **1b** was rather low: $k_{\text{ET}} = 1.8 \cdot 10^5 \text{ s}^{-1}$. In an operating system, such a rate would probably be too low to compete with back electron transfer. It is therefore important to prepare complexes where the ET rate from the manganese is higher. An obvious way of increasing the rate relative to

^[a] Dept. of Organic Chemistry, Stockholm University, 106 91 Stockholm, Sweden

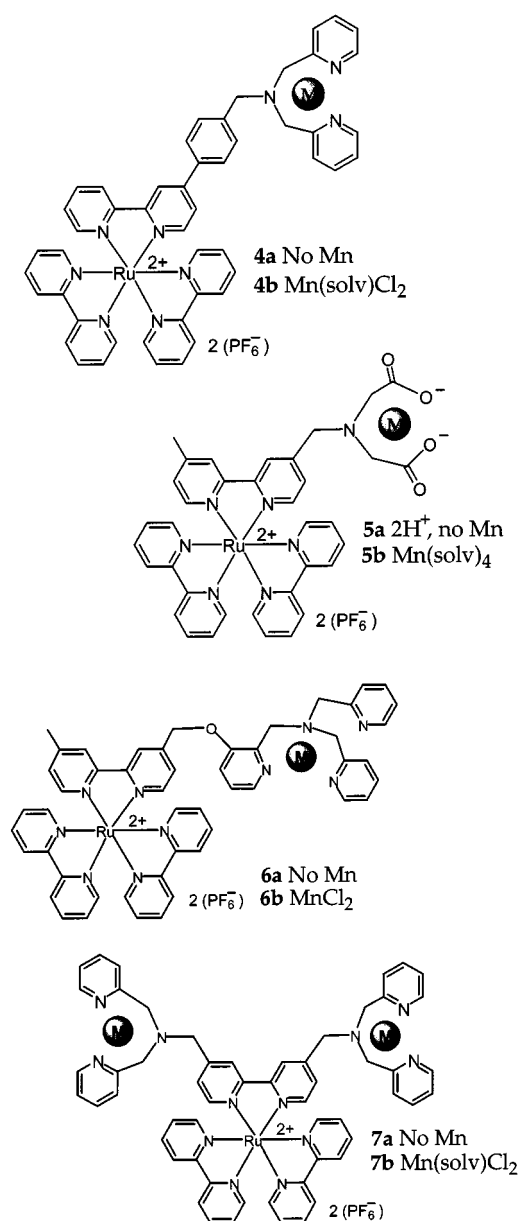
^[b] Dept. of Physical Chemistry, Uppsala University, Box 532, 751 21 Uppsala, Sweden

^[c] Dept. of Chemistry, Odense University, Campusvej 55, 5230 Odense M., Denmark

^[d] Dept. of Biochemistry, Center for Chemistry and Chemical Engineering, University of Lund, Box 124, 221 00 Lund, Sweden

complex **1b** is to decrease the Ru–Mn distance. This was estimated to be ca. 13 Å by using Chem 3D.^[6] The bispicene complex **2b**, which has an estimated Ru–Mn distance of ca. 9 Å, was therefore synthesized. However, because of quenching by the manganese, the lifetime of the excited state of this complex became so short, only 7 ns, that we were unable to observe electron transfer to the external acceptor, methylviologen.^[6] The Ru–Mn distance thus seemed very important for the functioning of the Ru sensitizer.

A study of the influence of this distance on the lifetime of the excited state of the ruthenium moiety and also on the rate of electron transfer from Mn to the photogenerated Ru^{III} clearly seems interesting. We therefore decided to synthesize a few binuclear Ru–Mn complexes with different Ru–Mn distances. In this paper, we describe complexes **3b–7b**, where manganese is coordinated to dipicolylamine (dpa), trispicolylamine (tpa), and aminodiacetic acid (ada).

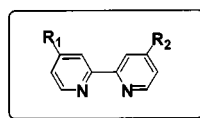


Dpa and tpa are known to bind manganese quite strongly.^[7–8] In complex **4b**, a tolyl spacer was inserted between the Mn ligand and the Ru center, and in **6b** a longer link was used. The lifetimes of the excited states, the intramolecular electron transfer rates, as well as the coordinating ability and the stability in solution are discussed and compared to those previously reported for complexes **1b** and **2b**.

Results

Synthesis and Characterization

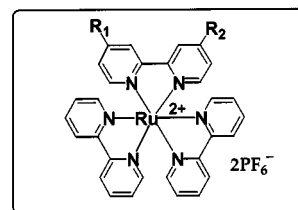
Two different strategies were used for the preparation of complexes **3b–7b**. In the synthesis of **5b**, ligand **8e** was obtained by the reaction of bromomethylbipyridine (**8b**) with iminodiacetic acid dimethyl ester.



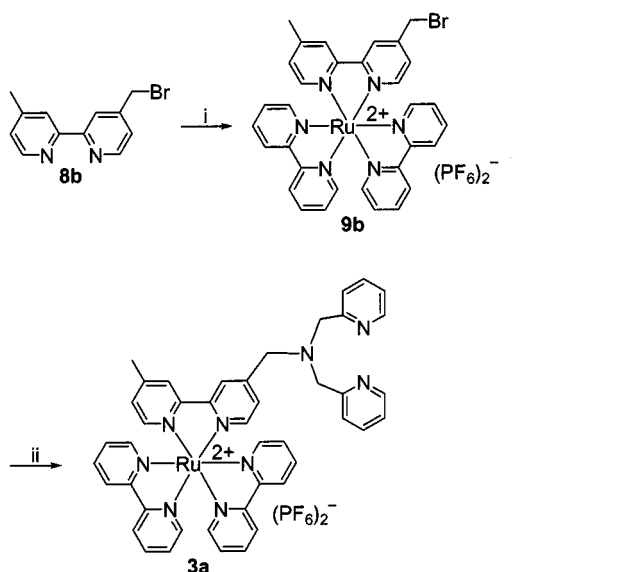
- 8a** R₁=CH₃, R₂=CH₂OH
8b R₁=CH₃, R₂=CH₂Br
8c R₁=R₂=CH₂OH
8d R₁=R₂=CH₂Br
8e R₁=CH₃, R₂=CH₂N(CH₂CO₂CH₃)₂

The ruthenium part was then introduced to give **10a**, which was hydrolyzed to **5a** and reacted with manganese(II). Complex **5b** could not be obtained in a pure form. In the synthesis of the other complexes, the ruthenium part was introduced before the ligand for manganese. Thus complexes **3b** and **7b** were prepared by the reaction of the ruthenium complexes **9b** and **9c** with dipicolylamine to give **3a** and **7a**, respectively, which were then treated with manganese(II) (Scheme 1). Complex **6b** was prepared in a similar way by the reaction of complex **9b** with the phenolic trispicolylamine **16** (Scheme 2).

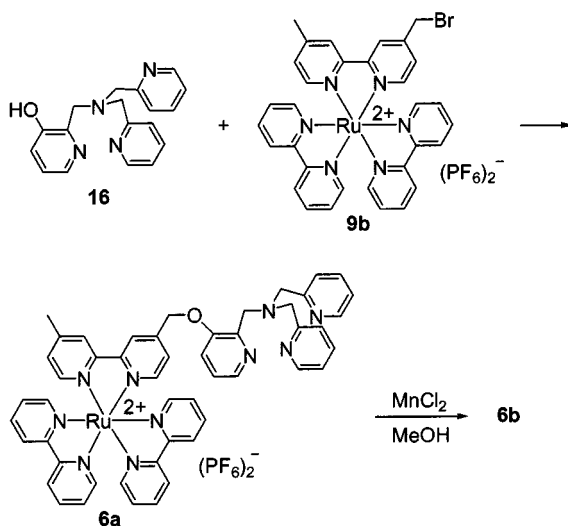
In the synthesis of complex **4b**, ligand **14** was first prepared by a classical polypyridine synthesis (Scheme 3). Tolualdehyde and pyruvate were condensed to give the ketoacid **11**, which after a second condensation with 2-pyridinyl pyridinium iodide and treatment with ammonia gave the



- 9a** R₁ = R₂ = H
9b R₁ = CH₃, R₂ = CH₂Br
9c R₁ = R₂ = CH₂Br
10a R₁ = CH₃, R₂ = —N(CH₂CO₂CH₃)₂



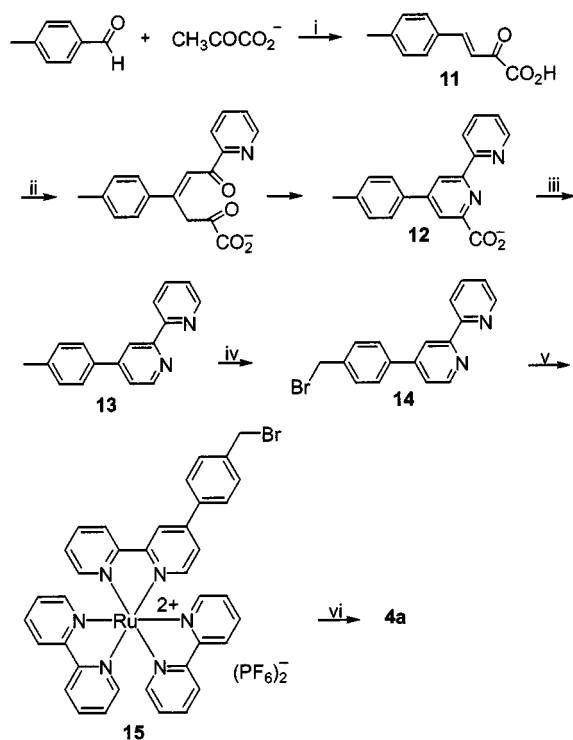
(i) $\text{Ru}(\text{bpy})_2\text{Cl}_2$, $\text{CF}_3\text{SO}_3\text{Ag}$, acetone; (ii) dipicolylamine, Et_3N , MeCN
Scheme 1



Scheme 2

ammonium carboxylate **12**. Decarboxylation by strong heating of the carboxylate in the absence of solvent gave the bipyridine **13**, which was brominated to give **14**. This was reacted with *cis*- $\text{Ru}(\text{bpy})_2\text{Cl}_2$ to give the ruthenium complex **15**, then with dipicolylamine to give **4a**, which was converted into the dinuclear Ru–Mn complex **4b** by treatment with MnCl_2 .

All new complexes in this paper, except **5b**, have been characterized using electrospray ionization mass spectroscopy (ESI-MS), ^1H NMR spectroscopy, and EPR spectroscopy. For manganese complexes, the NMR signals for the ruthenium moiety were generally observed as broadened peaks, whereas the signals for the manganese part could not be detected within a spectral width of 15 ppm.



(i) 1) EtOH , NaOH (10%), 2) HCl (2M); (ii) 2-pyridacyl pyridinium iodide, NH_4OAc , H_2O ; (iii) Δ ; (iv) NBS , AIBN , CCl_4 ; (v) $\text{Ru}(\text{bpy})_2\text{Cl}_2$, $\text{CF}_3\text{SO}_3\text{Ag}$, acetone; (vi) dipicolylamine, Et_3N , MeCN
Scheme 3

ESI-MS

In the ESI-MS spectra of complexes **3a**, **4a**, **5a**, **6a**, and **7a**, the singly-, doubly-, and/or triply charged species of the molecular ion were identified as the primary peaks of the spectra and are listed in the Experimental Section. Complexes **3b**, **4b**, **6b**, and **7b** gave rise to Mn-containing peaks, whereas **5b** gave a complicated pattern that could not be interpreted. The ESI-MS spectra of complexes **3b**, **4b**, **6b**, and **7b** in which Mn^{II} ions are incorporated into the ligands, contain numerous peaks from several species, differing by either the number of chlorides coordinated to manganese or by the presence of salt and/or solvent molecules held in the cavities. This apparent complexity clearly shows that manganese has been incorporated in the ligands.

EPR

The EPR spectra of solutions of the Ru–Mn complexes in MeOH/water (9:1) were recorded at 100 K. The very similar, jagged six-line spectra indicate that the coordination is very similar in the complexes **3b**, **4b**, **5b**, and **7b**. (Figure 1) The spectrum of **5b** is particularly interesting. Control experiments were conducted to exclude the possibility of Mn^{II} monomers or dimers bound to e.g. dissolved carbonate (CO_2 from the air). None of these control experiments showed spectra similar to those of the Ru–Mn complexes. In fact, when carbonate was added to a solution of $\text{Mn}^{\text{II}}\text{Cl}_2$, carbonate-bridging $\text{Mn}^{\text{II}}\text{--Mn}^{\text{II}}$ dimers were

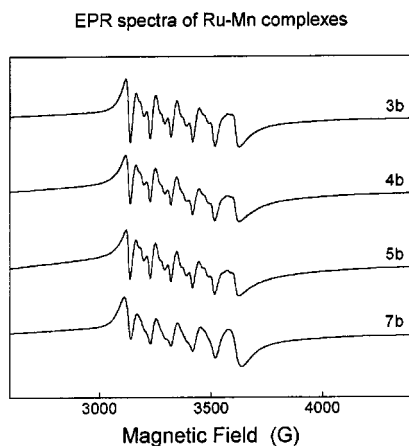


Figure 1. EPR spectrum showing the characteristic jagged 6-line trace for $\text{Ru}^{\text{II}}\text{--Mn}^{\text{II}}$ complexes (**3b**, **4b**, **5b**, and **7b**) in MeOH at 100 K

formed, yielding a broad spectrum with no hyperfine structure at 100 K.

Incorporation of manganese is rapid with bipyridyl and bispicen ligands,^[6] and slow with the tpa, dpa, and ada ligands. It could be shown that this was partly due to complexation of CO_2 by the free ligands. When the solution was bubbled with nitrogen before the introduction of manganese, the rate of its incorporation was greatly increased. When excess MnCl_2 was added, and the solution was allowed to equilibrate for several days, the coordination of manganese into the ligands approached 100% in complexes **3b**, **4b**, **5b**, and **7b**.

UV/Vis Spectroscopy

The UV/Vis absorption spectra of all the ruthenium tris-bipyridyl complexes were similar to those of the parent $\text{Ru}(\text{bpy})_3^{2+}$ complex (**9a**). Complexes **3a**, **4a**, **5a**, **6a**, and **7a** had the same absorption maxima (λ in nm): 245 (s), 253 (s), 287 (vs), and 453 (m) [for **9a**: 238, 259, 285, and 452 nm; for the dpa-ligand: 259 nm and a shoulder at 287 nm]. When manganese was coordinated into the ligand cavities of these complexes, thereby giving **3b**, **4b**, **5b**, **6b**, and **7b**, the absorption spectra were unchanged.

Emission Lifetimes and Quenching

The emission spectra of all complexes were typical of emission from the $^3\text{MLCT}$ state of $\text{Ru}(\text{bpy})_3^{2+}$ complexes, with corrected emission maxima for the compounds without Mn listed in Table 1. Upon binding of Mn, emission was quenched, the curves were somewhat broadened, and the maxima underwent a red-shift. Since much emission comes from the unquenched, manganese-free complexes, the values for the Ru–Mn complexes are uncertain in some cases. All complexes without manganese had excited-state lifetimes of approximately 1000 ns (1300 for **4a**). The emission lifetimes of the complexes with coordinated manganese were very short for complexes **3b** and **7b** (2.2 and 0.8 ns, respectively). The bispicene complex **2b**, which has a similar Ru–Mn distance, also has a short lifetime.^[6] The lifetime

Table 1. Photophysical data for complexes **1a–7a** and **10a**

Complex	Room temp. emission lifetime (fraction) τ [ns]	Room temp. corrected emission maximum λ [nm]	77 K corrected corrected emission maximum λ [nm]
1a	919	626	
2a	1050		
3a	880	640	585, 635, 697
4a	1300	629	588, 638, 699
5a	900	637	
6a		630	
7a	1090 (96%), 110 (4%) ^[a]	634	
10a	990		

[a] From reference [6]

of the ada complex **5b** was somewhat longer but because of poor coordination of manganese, the value is uncertain. For complexes **4b** and **6b**, which have approximately the same Ru–Mn distances as **1b**, it is interesting to note that the lifetime of **6b** was 120 ns, similar to that of **1b** (280 ns), but that of complex **4b** was only 23 ns (see Table 2).

The emission intensity of a 10 μM sample of **4b** in acetonitrile that was in a sealed, evacuated sample, remained constant over a period of 20 h. However, the emission of a second sample that was in a closed cuvette, but in acetonitrile saturated with air, increased to the level of the Mn-free complex **4a** with a half-life of 4 hours. Because the emission intensity is determined by the amount of bound manganese, this experiment demonstrated that atmospheric conditions promote manganese dissociation in this compound.

Flash Photolysis Studies

Electron-transfer reactions were studied by monitoring the transient absorptions of Ru^{II} species and the methylviologen radical ($\text{MV}^{\cdot+}$). The Ru^{III} species and MV^{2+} were generated by a laser flash which resulted in excitation of Ru^{II} followed by electron transfer to MV^{2+} , i.e. Equation (1).^[5a,6]



Since the formation of Ru^{III} occurred by means of a diffusion encounter of $\text{Ru}^{\text{II}*}$ with methylviologen, very high concentrations of MV^{2+} were necessary for compounds that have rapid intramolecular quenching of $\text{Ru}^{\text{II}*}$ by manganese (details in Experimental Section). This reaction was monitored by using the $\text{MV}^{\cdot+}$ absorption at approximately 600 nm, and the Ru^{II} ground-state bleaching at approximately 450 nm. In a subsequent reaction, the 450-nm absorption returned with a lifetime of the order of 1–10 μs , which we attributed to intramolecular electron transfer from the manganese [Equation (2)].



In contrast, the $\text{MV}^{\cdot+}$ absorption at 600 nm remained for more than 100 μs . It decayed in a second-order reaction

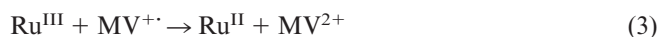
Table 2. Emission and electron-transfer data for Ru–Mn complexes and calculated Ru–Mn distances

Complex	Emission lifetime (fraction) τ [ns]	Ru–Mn complex ^[a] [%]	Electron transfer rate ^[b] [s ^{−1}]	Calculated Ru–Mn distance ^[c] [Å]
1b ^[d]	260	80	$1.8 \cdot 10^5$	13
2b ^[e]	7	93	—	9
3b	2.2	65	$1.3 \cdot 10^6$	9
4b	23	68	$1.6 \cdot 10^6$	14
5b	19 ^[f]	8	^[g]	9
6b	120	97	$1.3 \cdot 10^5$	14
7b	0.8 (76%), 2.9 (24%) ^[h]	94	^[g]	9
10b	—	0	^[g]	9

^[a] These percentages are from the fitting of the fluorescence decay curves of the Ru–Mn complexes. Each curve was fitted by a sum of two exponentials (three for **7b**), one exponential corresponding to the bound complex, and the other to the dissociated complex. Approximately 30 μM solutions of the 1:1 Ru–Mn complexes in acetonitrile were used. The percentages of bound complex are probably all concentration dependent. — ^[b] This is the half-life of the fastest component of the 450 nm Ru^{II} recovery. — ^[c] These are maximum Ru–Mn distances estimated by molecular mechanics starting from the most extended conformations using constrained metal–ligand distances. — ^[d] **1b** in acetonitrile (39 μM). From reference [6a]. — ^[e] **2b** in acetonitrile (67 μM). From reference [6a]. — ^[f] Determined with a twofold excess of MnCl₂ in acetonitrile, in order to obtain a larger fraction of attached Mn and thus a more reliable value. — ^[g] Not measured due to a low degree of Mn association or inability to quench the very short-lived excited state with methylviologen (see text). — ^[h] The fluorescence decay curve was fitted by a sum of two exponentials. This may be due to the presence of an impurity.

with $k_{ET} = 5 \cdot 10^9 \text{ M}^{-1}\text{s}^{-1}$, which we attributed to a diffusion-controlled recombination with the Mn^{III} species and some recombination with Ru^{III}.

When manganese was not present e.g. in **4a**, the 450 nm absorption and the 600 nm decay were mirror images, showing that the oxidized Ru^{III} regained an electron from the MV⁺⁺ in a recombination reaction that reformed the ground-state reactants [Equation (3)].



For **3a**, the Ru^{II} recovery at 450 nm was somewhat faster (first-order rate constant $k_{ET} \approx 1 \cdot 10^5 \text{ s}^{-1}$) owing to irreversible electron transfer from the dpa ligand, which leads to a build-up of MV⁺⁺. For **6a**, an even faster recovery was observed, $k_{ET} \geq 1 \cdot 10^7 \text{ s}^{-1}$, accompanied again by a build-up of MV⁺⁺. However, the ligands were stabilized against oxidation when Mn^{II} was coordinated. Thus, in **3b**, **4b**, and **6b** it was the Mn^{II} that was oxidized, and the MV⁺⁺ did not accumulate, presumably because it recombined with the Mn^{III} species (Figure 2). Complexes **3b** and **4b** displayed much faster Ru^{II} recovery than their Mn-free counterparts. In contrast, the recovery was much slower for **6b** (Figure 1) than for the manganese-free complex **6a**. The electron-transfer rate constants are summarized in Table 2.

Owing to partial dissociation of the Mn, the Ru^{II} recovery traces for **3b** and **4b** were fitted to a sum of two exponential processes, with a dominating fast recovery followed by a much slower one with smaller amplitude. The slower recovery rates agreed with measurements made with the Mn-free complexes. Only a small part of the slow recovery phase was seen on the timescale of the fast ET process [Equation (1)]. Therefore it could be represented by an exponential function in the fit, even though it was a second- or mixed first/second-order process.

For complex **6b**, a clean single-exponential first-order recovery of Ru^{II} was observed upon flash excitation in the

presence of MV²⁺. The rate constant ($1 \cdot 10^5 \text{ s}^{-1}$) was much lower than for complexes **3b** ($1.3 \cdot 10^6 \text{ s}^{-1}$) and **4b** ($1.6 \cdot 10^6 \text{ s}^{-1}$).

Cyclic Voltammetry

The half-wave potential ($E_{1/2}$) of the complexes **3a**, **3b**, **4a**, **4b**, **6a**, **6b**, and **9a** were determined by cyclic voltammetry (Table 3). For all the measured complexes, the peak split, ΔE_p , between the anodic (E_{pa}) and the cathodic (E_{pc}) peak potentials is less than 134 mV for the Mn^{III/II} peak and less than 84 mV for the Ru^{III/II} and the first reduction peak. The cyclic voltammograms of **4a** and **4b** are shown in Figure 3.

The reversible oxidation peak at approximately 1.30 V vs. SCE and the three reversible reduction peaks are typical of Ru^{III/II} oxidation and ligand reduction in Ru(bpy)₃²⁺ complexes. The irreversible oxidative peak for **4a** at approximately +1.1 V vs. SCE, also present for **3a**, was assigned to oxidation of the dpa ligand. When Mn^{II} was coordinated (**4b**), a reversible peak, which was assigned to the Mn^{III/II} couple, appeared at +0.90 V vs. SCE. Complexes **6a** and **6b** gave similar values for the corresponding peaks. Thus, the free energy changes (ΔG°) of electron transfer from Mn^{II} to Ru^{III} were −0.39 eV and −0.49 eV (ignoring work term corrections) for **4b** and **6b**, respectively. The Ru^{III/II} and the first ligand reduction potentials were very similar for **4a** and **4b**, and for **6a** and **6b**, showing that insertion of the neutral Mn^{II} complex only has a small coulombic effect on the ruthenium complex.

Discussion

Synthesis and Characterization

In the synthesis of complex **1b**, the bridging bipyridyl ligand was treated with *cis*-Ru(bpy)₂Cl₂ to give a mixture of mono- and diruthenium complexes, from which the mono-

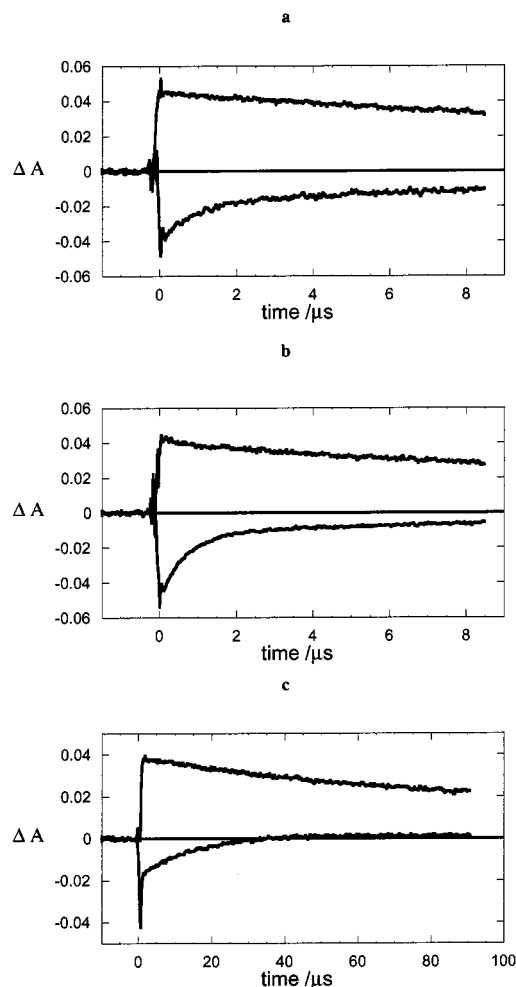


Figure 2. Transient absorption curves of Ru–Mn complexes (ca. $4 \cdot 10^{-5}$ M) with MV(PF₆)₂ in deoxygenated acetonitrile at room temperature: (a) **3b** with 0.30 M MV(PF₆)₂, (b) **4b** with 0.11 M MV(PF₆)₂, and (c) **6b** with 10 mM MV(PF₆)₂. It is worth noting that the relative contribution from the manganese-free fraction decreases regularly when going from (a) to (c). This is both due to an increasing degree in manganese binding, and to an increase in the excited-state lifetime for the Ru–Mn complex. Even with 0.30 M methyl viologen in (a), only a small part of the short-lived excited state of **3b** reacts, while the long-lived fraction of manganese-free complex present reacts quantitatively.

Table 3. Redox potentials determined by cyclic voltammetry in 0.1 M TBA·BF₄/CH₃CN at a glassy-carbon electrode (scan rate 100 mV/s). $E_{1/2}$ = redox half-way potential, $(E_{pa} + E_{pc})/2$

Complex	$E_{1/2}$ (Mn ^{III/II}) V vs. SCE	$E_{1/2}$ (Ru ^{III/II}) V vs. SCE	$E_{1/2}$ (ligand) V vs. SCE
3a	—	1.30	–1.32
3b	[a]	1.28	–1.31
4a	—	1.30	–1.27
4b	0.90	1.29	–1.28
6a	—	1.28	–1.32
6b	0.79	1.28	–1.31
Ru(bpy) ₃ ²⁺	—	1.32	–1.29

[a] The Mn^{III/II}-couple was not seen (see text).

complex could be isolated by chromatography. However, the substituted bipyridyl ligand in **2b** is unsymmetrical, and this strategy was therefore less attractive for the preparation

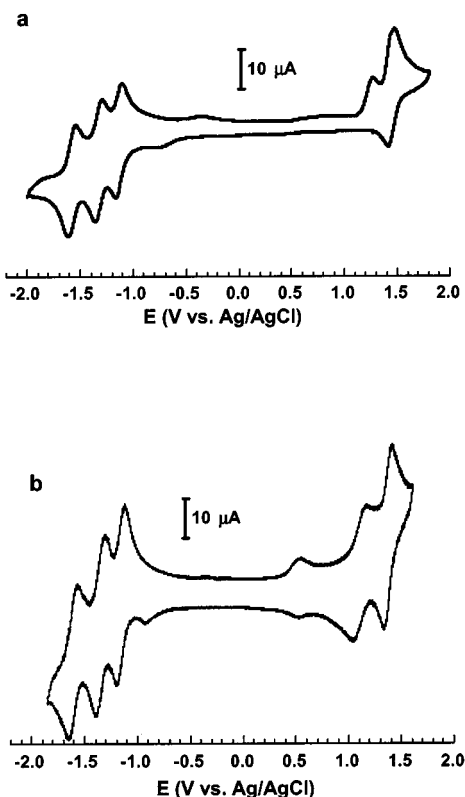


Figure 3. Cyclic voltammogram of (a) **4a** (0.92 mM) (b) **4b** (1.02 mM) in 0.1 M TBA·BF₄/MeCN at a glassy-carbon electrode. The small peak at ≈ 0.5 V vs. Ag/AgCl is due to an impurity present in the electrolyte which is adsorbed onto the electrode. The scan rate used is 100 mV/s

of this complex. Instead, the Ru^{II} trisbipyridyl moiety was prepared before introducing the ligand for manganese.^[6] Both strategies have been applied for the preparation of the complexes reported here. In the synthesis of **5b**, the ligand **8e** was first prepared and ruthenium could then be introduced selectively. Manganese could then be added after hydrolysis of the ester groups. In the synthetic routes to complexes **3b**, **4b**, **6b**, and **7b**, in which the final ligand could coordinate both ruthenium and manganese quite strongly, the intermediate ruthenium complexes **9b**, **9c**, and **15** were prepared first. As in the synthesis of **2b**, the ligand for manganese was then introduced, followed by manganese(II), to give the dinuclear complexes **3b**, **4b**, **6b**, and **7b**.

The EPR spectra of the Ru–Mn complexes all show essentially the same pattern (Figure 1). It can be concluded that the coordination geometry around manganese in the complexes is similar. Furthermore, the EPR spectra are identical whether the Mn^{II} is coordinated to an N- or to an O-donor; the patterns of the EPR spectra are mainly dependent on the coordination geometry around manganese.

With the exception of **5b**, the bipyridine ligand in **1b** is the weakest chelator for manganese of all the complexes described in this paper. The lifetime measurements show that in a dilute acetonitrile solution (ca. 30 μ M), approximately 30% of the manganese is dissociated in complexes **3b**, **4b**, and **7b**. This indicates stability similar to that of com-

plex **2b**. In contrast, only ca. 3% dissociation was observed with the tpa-complex **6b**. In aqueous solution, however, the coordinated manganese is rapidly lost from all the complexes **3b–7b**.

The bis-manganese complex **7b** gave a similar EPR spectrum as complex **3b**, suggesting the presence in **7b** of two nonbridging manganese(II) ions which do not interact. The molecular model of complex **7b** suggests that the two dpa moieties stretch away from each other in space owing to steric restriction, thus minimizing the likelihood of bridge formation between the two dpa units. An increase in the spacer length between the bipyridine and the dpa unit, or an uncoordinated bipyridine with free rotation about the bond between the pyridine rings would most probably allow for the formation of a Mn-oxo or Mn-acetato bridge.

The low rate of incorporation of manganese into the dpa cavity, as observed by EPR, could be due to the need to displace a molecule of CO₂, solvent, or ions already coordinated in the cavity. However, the introduction of a phenyl group to act as a rigid spacer between the Mn-coordinating ligand and the ruthenium entity did not change the coordination affinity for manganese: **3b** and **4b** have approximately the same amount of Mn dissociation (Table 2). Furthermore, the redox potential of Ru^{II} is the same in **4a**, in which manganese is absent, and in **4b**. This indicates that the weak coordination of manganese is mainly due to the nature of the ligand. The steady-state emission yield experiments (see Results section) demonstrated that Mn^{II} dissociated completely within hours in air-equilibrated solution, but that it remained bound in evacuated samples. This suggests that manganese is displaced either directly, for example by CO₂ in air, or indirectly as a result of oxidation of the dpa ligand.

Quenching of the Ru^{II}-Excited State by Manganese

Before coordination of manganese, the ruthenium complexes **1a–7a** have lifetimes of approximately 1000 ns, very similar to the lifetime of the parent bipyridine complex **9a**. On coordination of manganese, the lifetime is decreased, probably due to energy transfer by an exchange mechanism^[6b] involving the low-lying d–d states of the Mn^{II}. It would be expected that a short intermetallic distance would lead to more rapid quenching of the ruthenium excited state. The Ru–Mn distances determined by Chem 3D are summarized in Table 2. In general, complexes with shorter Ru–Mn distances (**3b**, **5b**, and **7b**) indeed have shorter emission lifetimes (Table 2). An exception is complex **4b**, which has an estimated Ru–Mn distance of ca. 14 Å but a lifetime of only 23 ns. This may be due to significant electron delocalization over the phenyl group.^[9] This would lead to a MLCT state that would be located more on the phenyl-substituted bipyridine. In contrast, complexes **1b** and **6b**, which have comparable Ru–Mn distances (13–14 Å), have much longer lifetimes: 260 ns and 120 ns, respectively.

The Ru^{II}* quenching rate constant in **7b** is almost double that of **3b**, which supports the suggestion that the two manganese units in **7b** act as independent moieties. The fact that

an additional exponent with a lifetime of 2.9 ns is needed to describe the decay in **7b** indicates that there may be a small fraction present where only one manganese atom is coordinated. The Mn-free complex **7a** also exhibits emission decay with a major ($\tau \approx 1000$ ns) and a very minor component (4% with $\tau \approx 100$ ns). Complex **6b** displays a distinct mono-exponential decay, in sharp contrast to the results obtained with complexes **3b–5b**.

Electron Transfer

The regeneration of the Ru^{II} sensitizer after photo-oxidation by methylviologen was very fast for **3b** and **4b** (Table 2). The reduction potentials show that electron transfer from Mn^{II} to Ru^{III} is energetically favorable, e.g. for **4b** $\Delta G^\circ = -0.39$ eV. Furthermore, the Ru^{II} recovery rates for **3b** and **4b** are much higher than those for the Mn-free complexes **3a** and **4a**. The measured Ru^{II} recovery rates are too high to be explained by a bimolecular reaction between Ru^{III} and Mn^{II} at the low concentrations (0.04 mM) employed. In addition, it could be shown that the rate constant for electron transfer was independent of the concentration for **4b**. We therefore attributed the Ru^{II} recovery in **3b** and **4b** to an intramolecular electron transfer from the Mn^{II} to the photogenerated Ru^{III}, in agreement with our previous reports on Ru–Mn complexes.^[6]

Similarly, intramolecular electron transfer is observed for complex **6b**. In this case, the rate constant is lower than for the manganese-free complex **6a**. However, in **6a** the ligand is the electron donor, but in **6b** it is the manganese ion, because the ligand is stabilized against oxidation after binding the metal. As a consequence, the electron transfer in **6b** is reversible, and the methylviologen radical is not accumulated. A possible reason for the rapid reaction of the amine in **6a** relative to **3a** could be that the longer link in the former could fold back towards the ruthenium. When the manganese atom is coordinated, the ligand is probably less flexible.

The electron-transfer rates for **3b** and **4b** are both nearly an order of magnitude faster than those observed for complexes **1b**^[6] and **6b**. The faster rate in **3b** is not surprising considering its shorter Ru–Mn distance. The rapid Mn^{II} to Ru^{III} electron transfer rate in **4b** however, was unexpected. Although the rate constant for electron transfer through phenylene spacers may decrease relatively slowly with distance,^[10] the fact that the Ru–Mn distance is 5 Å longer was expected to result in a much lower rate for **4b**. The high rate observed could be due to either a folding of the dpa unit or to conjugation through the phenylene spacer. The latter effect is perhaps the most probable since the spacer in **4a**, which has no manganese, has an influence both on the wavelength of the emission from the excited state of ruthenium (red shift of ca. 5 nm relative to **3a**) and on the lifetime of this state (1300 ns vs. 950 ns for **3a**).

Conclusions

A series of supramolecular complexes with a Ru(bpy)₃²⁺ core covalently linked to Mn-binding ligands have been pre-

pared and characterized. The coordinated manganese(II) was found to act as a strong quencher for the excited state of ruthenium, probably by energy transfer. In the absence of manganese, the excited-state lifetime of the $\text{Ru}(\text{bpy})_3^{2+}$ -type complexes was typically approximately 1000 ns. When the manganese ions were coordinated, the lifetimes were much shorter and there appeared to be a close relationship between the Ru–Mn distance and the emission lifetime. Thus the lifetimes of complexes **1b** and **6b**, in which the Ru–Mn distances were estimated to be 13–14 Å (by Chem 3D), were decreased to 255 and 120 ns, respectively. As the Ru–Mn distances were further shortened to ca. 9 Å, as in complexes **2b**, **3b**, and **7b**, the lifetimes became dramatically short: 7, 1.6, and 0.8 ns, respectively. The short lifetime of **4b**, (23 ns) in which the Ru–Mn distance is ca. 14 Å, is an exception which can be rationalized by delocalization of the excited state over the conjugated phenyl spacer.

Although we still have a fairly limited number of examples, the results so far seem to indicate that the rates of intramolecular electron transfer from manganese(II) to photo-generated ruthenium(III) also show some correlation with the Ru–Mn distances, increasing from ca. $1 \cdot 10^5 \text{ s}^{-1}$ for complexes **1b** and **6b** to $1.3 \cdot 10^6 \text{ s}^{-1}$ for complex **3b**.

In an artificial system, the electron transfer from manganese to the photo-generated ruthenium(III) must probably be fast in order to compete efficiently with back electron transfer from the acceptor. Our results suggest that this will be difficult with systems in which the manganese and ruthenium atoms are sufficiently close for rapid electron transfer because of the efficient quenching caused by the manganese atom. This problem presumably also exists in the natural PS II, where it has been solved by the insertion of a tyrosine unit (TyrosineZ) between the photosensitizer, chlorophyll P_{680} and the manganese cluster. This tyrosine unit then acts as an electron transfer relay. We have recently shown that a tyrosine group does not quench the excited state of Ru^{II} [11] and also that it can transfer an electron to the photo-oxidized ruthenium and recover it in an intramolecular reaction with a manganese(II)/(II) dimer. [12] In our future work we will therefore try to prepare supramolecular complexes in which a ruthenium(II) and a manganese(II) ion are linked by a tyrosine type unit.

Experimental Section

NMR, MS, and EPR: The ^1H NMR spectra were recorded on a Bruker AM400 MHz spectrometer or on a Bruker DMX500 MHz spectrometer, using TMS as internal standard. The electrospray ionization mass spectrometry (ESI-MS) experiments were performed on a TSQ700 (nanoES ion source) with acetonitrile or acetone as solvent. The EPR spectra were measured on a Bruker EMX spectrophotometer at 100 K using a 9:1 mixture of $\text{MeOH}/\text{H}_2\text{O}$ as solvent.

Absorption and Emission Measurements: Spectroscopic grade acetonitrile was used for all measurements. The UV spectra were measured on a Varian Cary 5E UV/Vis-NIR spectrophotometer. Emission spectra were recorded using a SPEX fluorolog II system. Emission lifetimes were determined by using time-correlated single

photon counting. The samples were purged with nitrogen gas and excited either at 327 nm by the frequency-doubled output from a YAG-pumped DCM dye laser, or at 400 nm by the frequency-doubled fundamental from a Ti-sapphire laser. A monochromator or interference filter centered at 610 nm was used to select the emission wavelength, which was detected with a microchannel plate. The two systems gave identical lifetimes within experimental error. The instrumental responses corresponded to four points or less out of 512 of the experimental decay curves and were not considered in the curve fitting.

Transient absorption studies were done by using an excimer laser pumping a Coumarin 47-dye laser to produce excitation pulses at 460 nm with a 15 ns width and an energy of 1 mJ/pulse at the sample. A pulsed Xe lamp provided analyzing light and the detection wavelengths were selected with a monochromator. All solutions were bubbled with nitrogen gas. The concentrations of the complexes were approximately 30 μM and that of methylviologen bis(hexafluorophosphate), $(\text{MV}(\text{PF}_6)_2)$, was 0.15–0.30 M in the studies of complexes **3b** and **4b**, and 10–20 mM for all other samples. The transient absorption curves were fitted to single- or double-exponential functions.

Cyclic Voltammetry: The electrolyte was a 0.1 M solution of tetrabutylammonium tetrafluoroborate ($\text{TBA} \cdot \text{BF}_4$, Aldrich) in acetonitrile. The $\text{TBA} \cdot \text{BF}_4$ was vacuum dried at 140 °C for 48 hours before use, and acetonitrile (Aldrich, 99.8%) was used as received. The glassware was cleaned, oven-dried, and transferred while hot to an argon filled glove box in which the experiments were performed.

A three-electrode system connected to an Eco Chemie model Autolab/GPES electrochemical interface was used. The working electrode was a freshly polished glassy-carbon disc (diameter 3 mm) and the counter electrode consisted of glassy carbon. The reference electrode was Ag/AgCl in LiCl saturated acetonitrile. Both the reference and the counter electrodes were separated from the solution by a salt bridge in contact with the working electrode.

The $E_{1/2}$ for **3a**, **3b**, **4a**, **4b**, **6b**, and $\text{Ru}(\text{bpy})_3(\text{Cl})_2$ (**9a**) were measured relative to a ferrocenium/ferrocene internal reference. The $E_{1/2}$ values are reported relative to SCE. The conversion was made by setting the $\text{Ru}^{\text{III/II}}$ value obtained for $\text{Ru}(\text{bpy})_3(\text{Cl})_2$ equal to 1.324 V relative to SCE. [13]

Materials: Azobis(isobutyronitrile) was recrystallized from EtOH. All other commercial reagents were used as obtained without further purification. Carbon tetrachloride was distilled from P_2O_5 prior to use. All other solvents were of HPLC grade (>99.7%) for synthesis or spectroscopic grade for optical measurements and were used as received. Silica gel 60 (230–400 mesh, Merck, Darmstadt, Germany) and neutral aluminum oxide gel (Aldrich) were used for column chromatography. The $\text{MV}(\text{PF}_6)_2$ was prepared by reacting 4,4'-bipyridine with MeI , then adding aqueous NH_4PF_6 to precipitate the PF_6 salt. The product was purified by recrystallization from EtOH.

4-Hydroxymethyl-4'-methyl-2,2'-bipyridine (8a): To a stirred suspension of 4,4'-dimethyl-2,2'-bipyridine (2.0 g, 11 mmol) in 1,4-dioxane (100 mL) was added SeO_2 (2.0 g, 18 mmol). The mixture was heated at reflux for 24 h. After cooling to room temperature, the mixture was filtered, and the solvent was removed under reduced pressure. The resulting pink solid was redissolved in chloroform, and the suspension was filtered to remove selenium by-products. After three successive dissolution and filtration treatments, crude product (1.4 g) was obtained. The resulting solid was suspended in methanol (15 mL), and sodium borohydride (0.3 g) in NaOH (0.2

m, 2.5 mL) was added dropwise to the stirred mixture cooled on ice. The mixture was stirred at room temperature for an additional hour and the methanol was then removed under reduced pressure. The remaining aqueous suspension was diluted with saturated Na_2CO_3 solution (6 mL) and extracted with chloroform. The organic phase was dried and the solvent evaporated. The crude product was purified by column chromatography (MPLC)^[14] to give 4-hydroxymethyl-4'-methyl-2,2'-bipyridine (1.2 g, 83%). All analytical data were in agreement with those reported by Geren et al.^[15]

4-Bromomethyl-4'-methyl-2,2'-bipyridine (8b): **8a** (1.0 g, 5.0 mmol) was dissolved in HBr (48%, 50 mL), and H_2SO_4 (conc., 2 mL) was added to the solution. The red solution was heated at reflux until all the starting material had been consumed as monitored by TLC (Al_2O_3 , hexane/EtOAc, 10:90). After the reaction had gone to completion (5–6 h), H_2O (13 mL) and CH_2Cl_2 (13 mL) were added. The aqueous layer was brought to pH 8 by adding saturated sodium carbonate solution and extracted with 10 mL portions of CH_2Cl_2 until the organic layer was colorless. The combined organic layers were dried with MgSO_4 and the CH_2Cl_2 removed in vacuo to yield 4-bromomethyl-4'-methyl-2,2'-bipyridine (**8b**) (1.3 g, 98% yield). All analytical data were in agreement with those previously reported.^[6]

$\text{Ru}(\text{bpy})_2(4\text{-bromomethyl-4'-methylbipyridine})(\text{PF}_6)_2$ (9b**):** Complex **9b** was isolated and characterized as reported earlier by Sun et al.^[6]

$\text{Ru}(\text{bpy})_2[4\text{-(dpa-CH}_2\text{)-4'-methylbipyridine}](\text{PF}_6)_2$ (3a**):** Dipicolylamine^[16] (0.015 g, 0.073 mmol) and Et_3N (1 equiv.) were dissolved in acetonitrile and added dropwise to a solution of $\text{Ru}(\text{bpy})_2(4\text{-bromomethyl-4'-methylbipyridine})(\text{PF}_6)_2$ (**9b**) (0.071 g, 0.073 mmol) in acetonitrile. The reaction mixture was heated at reflux under argon for 3 h, then cooled and filtered. The filtrate was evaporated in vacuo and the product was purified by chromatography (MPLC)^[14] (silica gel, MeCN/water/ KNO_3 (sat.), 28:1:2). The desired product eluted as the second band and excess KNO_3 was removed by filtration after dissolving the product in acetone. Water and NH_4PF_6 were added to a MeOH solution of the product to afford a red–orange product which was collected by filtration, washed and dried to yield $\text{Ru}(\text{bpy})_2[4\text{-(dpa-CH}_2\text{)-4'-methylbipyridine}](\text{PF}_6)_2$ (**3a**) (0.042 g, 53%). – ^1H NMR ($[\text{D}_6]\text{acetone}$): δ = 2.58 (s, 3 H, Mebpy CH_3), 4.37 (s, 2 H, Mebpy CH_2N^-), 4.49 (s, 4 H, dpa CH_2N^-), 7.37–7.42 (m, 1J = 6 Hz, 1 H, Mebpy $\text{Py}'\text{-H}$), 7.50–7.55 (m, 3 H, bpy Py-H), 7.52–7.58 (m, 1J = 6 Hz, 1 H, Mebpy Py-H), 7.64–7.68 (m, 1 H, bpy Py-H), 7.67–7.72 (m, 4 H, dpa Py-H), 7.77 (d, 1J = 6 Hz, 1 H, Mebpy Py-H), 7.83 (d, 1J = 6 Hz, 1 H, Mebpy $\text{Py}'\text{-H}$), 7.85 (ddd, 1 H, bpy Py-H), 7.99 (d, 1J = 5 Hz, 2 H, bpy Py-H), 8.02 (ddd, 1 H, bpy Py-H), 8.14 (dd, 2 H, dpa Py-H), 8.18 (ddd, 1 H, bpy Py-H), 8.19 (ddd, 2 H, bpy Py-H), 8.26 (ddd, 1 H, bpy Py-H), 8.58 (s, 1 H, Mebpy $\text{Py}'\text{-H}$), 8.75 (s, 1 H, Mebpy Py-H), 8.79 (d, 1J = 8 Hz, 3 H, bpy Py-H), 8.83 (d, 1J = 8 Hz, 1 H, bpy Py-H), 9.02 (d, 1J = 5 Hz, 2 H, dpa Py-H). – ESI-MS (m/z): 1086.2 [$\text{M} + \text{H}^+$], 940.2 [$\text{M} - \text{PF}_6^-$], 398.0 [$\text{M} - 2\text{PF}_6^-$].

2-Oxo-4-(tolyl)but-3-enoic Acid (11): This compound was prepared by a method described by Baba et al.^[17] To a solution of sodium pyruvate (8.3 g, 0.075 mol) in water (15 mL) cooled in an ice bath, was added tolaldehyde (6.0 g, 0.050 mol) dissolved in EtOH (85 mL). To this rapidly stirred mixture was added NaOH (10% w/w, 30 mL). After stirring for an additional 15 min, the mixture was acidified with HCl (2 M), and stirred for 5 min. The yellow precipitate was filtered and washed with water and EtOH, and dried to give the acid **11** (4.9 g, 52%). – ^1H NMR ($[\text{D}_6]\text{DMSO}$): δ = 2.33 (s, 3 H, –phenyl CH_3), 6.70 (d, 1 H, – $\text{HC}=\text{CHCO}-$), 7.23 (d, 2 H, phenyl– H), 7.40 (d, 1 H, – $\text{HC}=\text{CHCO}-$), 7.53 (d, 2 H, phenyl– H).

4-(*p*-Tolyl)-2,2'-bipyridine (13): This compound was prepared by a modification of the method described by Baba et al.^[17] A suspension of the acid **11** (4.0 g, 0.021 mol), 2-pyridacylpyridinium iodide^[18] (9.7 g, 0.030 mol) and ammonium acetate (16 g, 0.21 mol) in water (150 mL) was heated at reflux for 3 h. The resulting precipitate was filtered from the hot solution and washed with water and dried to yield the ammonium salt of 4-(*p*-tolyl)-2,2'-bipyridine-6-carboxylic acid (**12**) (3.5 g, 53%). Mp: 181 °C (uncorr.). – ^1H NMR ($[\text{D}_6]\text{DMSO}$): δ = 2.39 (s, 3 H, –phenyl CH_3), 7.37 (d, 1J = 8 Hz, 2 H, phenyl– H), 7.48 (dd, 1J = 8 Hz, 5 Hz, 1 H, $\text{Py}'\text{-H}$), 7.76 (d, 1J = 8 Hz, 2 H, phenyl– H), 7.98 (t, 1J = 8 Hz, 1 H, $\text{Py}'\text{-H}$), 8.14 (s, 1 H, Py-H), 8.50 (d, 1J = 8 Hz, 1 H, $\text{Py}'\text{-H}$), 8.58 (s, 1 H, Py-H), 8.72 (d, 1J = 5 Hz, 1 H, $\text{Py}'\text{-H}$).

The ammonium salt **12** (2.0 g, 6.5 mmol) was gently heated over a Bunsen flame until evolution of CO_2 had ceased. The solution was cooled, suspended in Et_2O , and stirred in the presence of activated charcoal for 15 min. Filtration and evaporation of the solvent gave a brown solid (1.2 g). Column chromatography (Al_2O_3 , $\text{CH}_2\text{Cl}_2/\text{EtOH}$, 9:1) gave 4-(*p*-tolyl)-2,2'-bipyridine (tolbpy) (1.0 g, 38%) as a pale yellow powder. Mp: 112 °C (uncorr.). – ^1H NMR ($[\text{D}_6]\text{DMSO}$): δ = 2.39 (s, 3 H, –phenyl CH_3), 7.38 (d, 2 H, phenyl– H , J = 8 Hz), 7.49 (dd, 1 H, $\text{Py}'\text{-H}$, J = 8 Hz, 5 Hz), 7.75 (d, 1 H, $\text{Py}'\text{-H}$, J = 5 Hz), 7.78 (d, 2 H, phenyl– H , J = 8 Hz), 7.98 (t, 1 H, $\text{Py}'\text{-H}$, J = 8 Hz), 8.45 (d, 1 H, $\text{Py}'\text{-H}$, J = 8 Hz), 8.66 (s, 1 H, Py-H), 8.73 (d, 2 H, Py-H and $\text{Py}'\text{-H}$, J = 5 Hz). MS (EI) (m/z): 246.2 [M^+].

4-[*p*-(Bromomethyl)phenyl]-2,2'-bipyridine (14): A solution of *p*-tolbpy (**13**) (0.5 g, 2.0 mmol), *N*-bromosuccinimide (0.4 g, 2.0 mmol), and azobis(isobutyronitrile) (0.010 g, 0.065 mmol) in dry CCl_4 (20 mL) was heated at reflux for 19 h under argon. The cooled reaction mixture was filtered. On removal of the solvent, a yellow oil was obtained which soon crystallized to give a yellow solid (0.58 g, 88% yield). This crude product was used in the next reaction without further purification. A peak at δ = 4.6 (CDCl_3) in the NMR spectrum was identified as the methylene protons between the bromine and the phenyl group.

$\text{Ru}(\text{bpy})_2\{[4\text{-(*p*-bromomethyl)phenyl]-2,2'-bipyridine}\}(\text{PF}_6)_2$ (15**):** A solution of *cis*- $\text{Ru}(\text{bpy})_2\text{Cl}_2 \cdot 2\text{H}_2\text{O}$ ^[19] (0.89 g, 1.7 mmol) and silver triflate (0.89 g, 3.5 mmol) in anhydrous acetone (65 mL) was stirred for 15 h at room temperature under argon and protected from light. The precipitated AgCl was removed by filtration, and compound **14** (0.55 g, 1.7 mmol) was added to the red filtrate. This reaction mixture was stirred in the dark at room temperature for 6 h under an argon atmosphere. The acetone was evaporated and the red residue was dissolved in a mixture of MeOH (15 mL) and water (25 mL). The ruthenium complex was precipitated from the solution by addition of concentrated NH_4PF_6 . The red–brown precipitate was collected by suction filtration and washed with water. Purification by column chromatography (MPLC)^[14] (Al_2O_3 , $\text{CH}_2\text{Cl}_2/\text{EtOH}$, 95:5) afforded the red complex (0.50 g, 29% yield). – ^1H NMR ($[\text{D}_6]\text{acetone}$): δ = 4.76 (s, 2 H, –phenyl CH_2Br), 7.59–7.64 (m, 5 H, $\text{Py}'\text{-H}$ and $\text{Py}''\text{-H}$), 7.71 (d, 1J = 8 Hz, 2 H, phenyl– H), 7.91 (dd, 1J = 7 Hz, 2 Hz, 1 H, Py-H), 7.99 (d, 1J = 8 Hz, 2 H, phenyl– H), 8.10–8.12 (m, 5 H, Py-H and $\text{Py}''\text{-H}$), 8.19 (d, 1J = 5 Hz, 1 H, $\text{Py}'\text{-H}$), 8.24–8.28 (m, 5 H, $\text{Py}'\text{-H}$ and $\text{Py}''\text{-H}$), 8.88 (d, 1J = 6 Hz, 4 H, $\text{Py}''\text{-H}$), 9.13 (d, 1J = 8 Hz, 1 H, $\text{Py}'\text{-H}$), 9.18 (d, 1J = 2 Hz, 1 H, Py-H).

$\text{Ru}(\text{bpy})_2\{[4\text{'-}[4\text{-bis(2-methylpyridine)aminomethyl}]\text{phenyl}]\text{bipyridine}\}(\text{PF}_6)_2$ (4a**):** Compound **15** (0.084 g, 0.082 mmol) and dipicolylamine^[16] (0.021 g, 0.11 mmol) were dissolved in acetonitrile (2 mL). After the addition of 3 drops of Et_3N , the solution was

heated at reflux for 7 h. The solvent was evaporated and the resulting residue was purified by column chromatography on silica gel using MeCN/water/KNO₃(sat.) (28:1:2) as eluent to afford the pure product (0.019 g, 20%). – ¹H NMR ([D₆]acetone): δ = 3.89 (s, 2 H, phenylCH₂N–), 3.91 (s, 4 H, dpaCH₂N–), 7.30 (dd, ¹J = 5 Hz, 2 H, dpaPy–H), 7.56–7.62 (m, 5 H, bpyPy–H (4 H) and tolbpPy–H (1 H)), 7.68 (d, ¹J = 7 Hz, 2 H, dpaPy–H), 7.71 (d, ¹J = 9 Hz, 2 H, phenyl–H), 7.82 (dt, ¹J = 7 Hz, 2 Hz, 2 H, dpaPy–H), 7.87 (dd, ¹J = 6 Hz, 2 Hz, 1 H, tolbpPy–H), 7.96 (d, ¹J = 9 Hz, 2 H, phenyl–H), 8.06 (d, ¹J = 6 Hz, 1 H, tolbpPy–H), 8.07–8.11 (m, 4 H, bpyPy–H), 8.15 (d, ¹J = 6 Hz, 1 H, tolbpPy–H), 8.19–8.25 (m, 5H; bpyPy–H (4 H) and tolbpPy–H (1 H)), 8.57 (d, ¹J = 5 Hz, 2 H, dpaPy–H), 8.85 (d, ¹J = 8 Hz, 4 H, bpyPy–H), 9.12 (d, ¹J = 9 Hz, 1 H, tolbpPy–H), 9.13 (s, 1 H, tolbpPy–H). – ESI-MS (*m/z*): 1002.3 [M – PF₆][–], 501.3 [M – PF₆ + H]⁺, 428.3 [M – 2 PF₆][–].

4-[Bis(methyl acet-2-yl)aminomethyl]-4'-methyl-2,2'-bipyridine (8e): The hydrochloride salt of iminodiacetic acid dimethyl ester (0.44 g, 2.4 mmol) and anhydrous sodium carbonate (1.0 g) were dissolved in acetonitrile (150 mL). 4-Bromomethyl-4'-methyl-2,2'-bipyridine (**8b**) (0.63 g, 2.4 mmol) was added and the reaction was stirred for 10 h at 4 °C. After heating at reflux overnight, the reaction mixture was cooled and filtered. The solid was washed with ethyl acetate and the solvent evaporated under reduced pressure. The crude dark red product was purified on silica gel using ethyl acetate as eluent. The desired product was obtained as an uncolored oil (0.57 g, 76%). – ¹H NMR (CDCl₃): δ = 2.43 (s, 3 H, bpyCH₃), 3.59 (s, 4 H, CH₂COO), 3.70 (s, 6 H, ester OCH₃), 4.04 (s, 2 H, bpyCH₂), 7.12 (d, 1 H, bpyPy–H), 7.48 (d, 1 H, bpyPy–H), 8.22 (s, 1 H, bpyPy–H), 8.33 (s, 1 H, bpyPy–H), 8.54 (d, ¹J = 5 Hz, 1 H, bpyPy–H), 8.64 (d, ¹J = 5 Hz, 1 H, bpyPy–H).

Ru(bpy)₂[4-[CH₂N(CH₂COOH)₂]-4'-methylbipyridine](PF₆)₂ (5a): Hydrolysis of ester **10a** in a NaOH/H₂O solution overnight gave the desired diacid **5a** in quantitative yield. – ¹H NMR (D₂O): δ = 2.50 (s, 3 H, MebpyCH₃), 3.21 (s, 4 H, –NCH₂COOH), 3.90 (s, 2 H, MebpyCH₂N–), 7.24 (d, 1 H, MebpyPy–H), 7.32–7.43 (m, 4 H, bpyPy–H), 7.46 (d, 1 H, MebpyPy–H), 7.63 (d, 1 H, MebpyPy–H), 8.00–8.06 (m, 4 H, bpyPy–H), 8.43 (s, 1 H, MebpyPy–H), 8.51 (d, 4 H, bpyPy–H), 8.60 (s, 1 H, MebpyPy–H). – ESI-MS (*m/z*): 874.3 [M – PF₆][–], 364.2 [M – 2 PF₆][–].

{2-[(Dipicolyl)aminomethyl]-3-hydroxypyridine (16): 2-Bromomethyl-3-hydroxypyridine hydrobromide (3.8 g, 0.014 mol), obtained according to a literature procedure^[20] was added over a period of 3 h, to a refluxing solution of dipicolylamine^[16] (2.8 g, 0.014 mol) in MeCN (400 mL), containing sodium carbonate (10 g). The mixture was heated at reflux overnight, cooled, and purified by column chromatography on silica gel, using CH₂Cl₂/MeOH (94:6) as eluent, to give compound **16** (HO-tpa) in 78% yield. ¹H NMR (CDCl₃): δ = 7.16 (d, ¹J = 2.6 Hz, 2 H), 7.25 (m, 2 H), 7.37 (d, ¹J = 8.6 Hz, 2 H), 7.72 (td, ¹J = 8.6 Hz, 1.2 Hz, 2 H), 7.92 (m, 1 H), 8.47 (d, ¹J = 4.8 Hz, 2 H). – ¹³C NMR (CDCl₃): δ = 123.0, 123.3, 123.5, 124.4, 137.5, 139.7, 144.6, 149.0, 153.6, 158.3. – ESI-MS (*m/z*): 306 [M]⁺.

Ru(bpy)₂[4-(CH₂O-tpa)-4'-methylbipyridine](PF₆)₂ (6a): Metallic sodium (3.1 mg) was dissolved in dry MeOH (5 mL), and **16** (HO-tpa) (0.041 g, 1.35 mmol) was added followed by DMSO (4 mL). MeOH was evaporated under reduced pressure. Ru(bpy)₂(4-bromomethyl-4'-methylbipyridine)(PF₆)₂ (**9b**, 0.13 mg) was added and the mixture was heated at 80 °C for 4 d in the dark. DMSO was removed under vacuum and the resulting product was purified by chromatography (silica gel, MeCN/water/KNO₃(sat.), 7:1:1). The

compound was precipitated by the addition of saturated NH₄PF₆ (aq.) and purified further by MPLC^[14] on aluminum oxide using CH₂Cl₂/MeOH (95:5) to give compound **6a** in 46% yield. – ¹H NMR ([D₆]acetone): δ = 2.53 (s, 3 H, bpyCH₃), 3.96 (s, 4 H, pyCH₂N–), 4.07 (s, 2 H, pyCH₂N–), 5.42 (s, 2 H, bpyOCH₂–), 7.06 (m, 2 H, py–H), 7.24 (m, 1 H, py–H), 7.43 (m, 2 H, py–H), 7.56–7.65 (m, 9 H, py–H), 7.87 (d, ¹J = 5.8 Hz, 1 H, Mebpy–H), 7.98–8.10 (m, 6 H, py–H), 8.18–8.24 (m, 5 H, py–H), 8.33 (d, ¹J = 6.0 Hz, 1 H, Mebpy–H), 8.69 (s, 1 H, Mebpy–H), 8.82 (m, 4 H, bpy–H), 8.94 (s, 1 H, Mebpy–H). – ESI-MS (*m/z*): 1046 [M – PF₆][–], 450 [M – 2 PF₆][–].

[4,4'-Bis(bromomethyl)]-2,2'-bipyridine (8d): Compound **8d** was prepared via the diol **8c** in the same manner as **8b**, but with a large excess of SeO₂ to oxidize the dimethylbipyridine and 2 mol equivalents of NaBH₄ to reduce the dialdehyde. Due to problems with hydrolysis during attempted purification of this ligand, the crude product was used directly in the following step.

Ru(bpy)₂[4,4'-bis(CH₂Br)bpy](PF₆)₂ (9c): *cis*-Ru(bpy)₂Cl₂ · 2 H₂O^[19] (0.10 g, 0.20 mmol) and silver triflate (2 equiv.) were dissolved in anhydrous acetone. The mixture was stirred for 7 h at room temperature under argon. The AgCl that formed during the reaction was removed by filtration. [4,4'-Bis(bromomethyl)]-2,2'-bipyridine (**8d**) (0.068 g, 0.20 mmol) was added to the filtrate and the reaction mixture was allowed to stir at room temperature under argon. After 1.5 h, the solvent was evaporated under reduced pressure and the red product was redissolved in MeOH. The product was precipitated by the addition of concentrated aqueous NH₄PF₆. The resulting product was purified by column chromatography (MPLC)^[14] on neutral Al₂O₃, gradient elution, EtOH/CH₂Cl₂, 0:100 to 10:90, to afford Ru(bpy)₂[4,4'-bis(CH₂Br)-bpy](PF₆)₂ (**9c**) (0.072 g, 35% yield).

Ru(bpy)₂[4,4'-bis(CH₂-dpa)bpy](PF₆)₂ (7a): A solution of dipicolylamine^[16] (0.028 g, 0.14 mmol) and Et₃N (slight excess) was added dropwise to a solution of **9c** (0.072 g, 0.069 mmol) in MeCN. The reaction was allowed to stir for 7 h under argon. The solvent was removed under reduced pressure and the product was purified by column chromatography (silica gel, MeCN/water/KNO₃(sat.), 28:1:2). The desired product was eluted as the second band and excess KNO₃ was removed by filtration after dissolving the product in acetone. The product was then precipitated from a MeOH/water solution by adding concentrated aqueous NH₄PF₆ to yield **7a** (0.070 g, 79%). – ¹H NMR (CDCl₃): δ = 3.94 (s, 8 H, dpaCH₂N–), 4.08 (s, 4 H, bpyCH₂N–), 7.19–7.22 (ddd, 4 H, dpaPy–H), 7.50 (dd, 4 H, dpaPy–H), 7.52–7.55 (m, 4 H, bpyPy–H), 7.65 (d, 2 H, bpyPy–H), 7.66 (d, 2 H, bpyPy–H), 7.66–7.71 (ddd, 4 H, dpaPy–H), 7.74–7.76 (dd, 4 H, bpyPy–H), 8.14–8.17 (m, 4 H, bpyPy–H), 8.58 (dd, 4 H, dpaPy–H), 8.91 (s, 2 H, bpyPy–H), 9.11–9.14 (dd, 4 H, bpyPy–H). – ESI-MS (*m/z*): 495.8 [M – 2 PF₆][–], 331.1 [M – 2 PF₆ + H]⁺.

Ru(bpy)₂[4-[CH₂N(CH₂CO₂CH₃)₂]-4'-methylbipyridine](PF₆)₂ (10a): *cis*-Ru(bpy)₂Cl₂ · 2 H₂O^[19] (0.89 g, 1.8 mmol) and **8e** (0.60 mg, 1.8 mmol) were dissolved in MeOH (200 mL) and heated at reflux overnight. The solvent was removed and water (80 mL) was added. After filtration of the red solution, a large excess of NH₄PF₆ (1.0 g) was added to the filtrate and the orange precipitate was collected by filtration, washed with water and dried to yield **10a**. The product was purified by column chromatography (MPLC)^[14] (Al₂O₃, CH₂Cl₂/EtOH, 97:3) and obtained in 65% yield. – ¹H NMR ([D₆]acetone): δ = 2.64 (s, 3 H, MebpyCH₃), 3.67 (s, 6 H, –COOCH₃), 3.72 (s, 4 H, –NCH₂COOCH₃), 4.25 (s, 2 H, MebpyCH₂), 7.48 (d, 1 H, MebpyPy–H), 7.61–7.67 (m, 4 H, bpyPy–H), 7.71 (d, 1 H,

MebpyPy–H), 7.92 (d, 1 H, MebpyPy'–H), 8.00 (d, 1 H, MebpyPy–H), 8.06–8.15 (m, 4 H, bpyPy–H), 8.23–8.29 (m, 4 H, bpyPy–H), 8.46 (s, 1 H, MebpyPy'–H), 8.88 (d, 4 H, bpyPy–H), 8.92 (s, 1 H, MebpyPy–H). – ESI-MS (*m/z*): 902.3 [M – PF₆[–]], 378.1 [M – 2 PF₆[–]].

Ru(bpy)₂[4-(CH₂-O-tpa-Mn)-4'-methylbipyridine](PF₆)₂ (6b): MnCl₂ · 4 H₂O (0.030 g, 0.15 mmol) was added to compound **6a** (0.12 g, 0.10 mmol) dissolved in MeOH (10 mL). After 10 min, a concentrated aqueous solution of NH₄PF₆ was added and a red precipitate was formed after 5 min of stirring at room temperature. Filtration and washing with cold MeOH and Et₂O, followed by drying gave **6b** as a red solid (0.11 g, 83% yield). – ¹H NMR ([D₆]acetone): proton signals from the ligands in the ruthenium moiety were broadened, and proton signals for the manganese ligands were not seen when using a spectral width of 15 ppm. – ESI-MS (*m/z*): 1175 [M – PF₆[–]], 567 [M – PF₆[–] – Cl[–]], 514 [M – 2 PF₆[–]], 331 [M – 2 PF₆[–] – Cl[–]].

The Mn complexes **3b**, **4b**, **5b**, and **7b** were prepared in a similar way as **6b**, except that the reaction times with MnCl₂ varied from a few hours to two days. After the addition of NH₄PF₆, filtration and drying, the complexes **3b**, **4b**, **5b**, and **7b** were obtained as fine powders. Complex **5b** was only obtained in an impure state and was not fully characterized.

Ru(bpy)₂(bpy-dpaMn)(PF₆)₂Cl₂ (3b): ESI-MS (*m/z*): 569.8 [M – 2 Cl[–]], 533.3 [M – PF₆[–] + H⁺], 514.5 [M – PF₆[–] – Cl[–]], 460.3 [M – 2 PF₆[–]].

Ru(bpy)₂(bpy-tolyl-dpaMn)(PF₆)₂Cl₂ (4b): ESI-MS (*m/z*): 1127.2 [M – PF₆[–]], 600.7 [M – 2 Cl[–]], 545.7 [M – PF₆[–] – Cl[–]], 315.5 [M – 2 PF₆[–] – Cl[–]].

Ru(bpy)₂(bpy-bisdpaMn₂)(PF₆)₂Cl₄ (7b): ESI-MS (*m/z*): 749.3 [M – Cl[–] + H⁺], 731.2 [M – 2 Cl[–]], 676.9 [M – PF₆[–] – Cl[–]].

Acknowledgments

The financial support for this work was provided by the Nordic Energy Research Council, the Knut and Alice Wallenberg Foundation, the Swedish Research Council for Engineering Sciences, the Swedish Natural Science Research Council, and the European TMR Program (TMR Network CT 96-0031). We are also very thankful to Jens Z. Pedersen for recording the EPR spectra, Tina Esbech for measuring the ESI-MS spectra, and Daniel Czermac for contributions to the synthesis.

[1] For recent general reviews, see e. g.: [1a] A. J. Bard, M. A. Fox, *Acc. Chem. Res.* **1995**, *28*, 141. – [1b] E. Amouyal, *Sol. Energy Mater. Sol. Cells* **1995**, *38*, 249.

[2] [2a] R. D. Britt, In *Oxygenic Photosynthesis: The Light Reactions* (Eds. D. R. Ort, C. F. Yocum), Kluwer Academic, Dordrecht, Netherlands, **1996**, p. 137. – [2b] V. K. Yachandra, M. P. Sauer, M. P. Klein, *Chem. Rev.* **1996**, *96*, 2927. – [2c] R. J. Debus, *Biochim. Biophys. Acta* **1992**, *269*, 1102. – [2d] G. W. Brudvig, *Mechanistic Bioinorganic Chemistry: Advances in Chemistry Ser. 246* (Eds. H. H. Thorp, V. L. Pecoraro), ACS Washington DC, **1995**, p. 249.

[3] [3a] J. Limburg, V. A. Szalai, G. W. Brudvig, *J. Chem. Soc., Dalton Trans.* **1999**, 1353. – [3b] P. E. M. Siegbahn, R. H. Crabtree, *J. Am. Chem. Soc.* **1999**, *121*, 117. – [3c] G. Blöndin, R. Davydov, C. Philouze, M.-F. Charlot, S. Styring, B. Åkermark, J.-J. Girerd, A. Boussac, *J. Chem. Soc., Dalton Trans.* **1997**, 4069. – [3d] V. K. Yachandra, V. J. DeRose, M. J. Latimer, I. Mukerji, K. Sauer, M. P. Klein, *Science* **1993**, *260*, 675.

- [4] [4a] W. Rüttinger, C. G. Dismukes, *Chem. Rev.* **1997**, *97*, 1. – [4b] S. Pal, M. K. Chan, W. H. Armstrong, *J. Am. Chem. Soc.* **1992**, *114*, 6398. – [4c] R. Manchanda, G. W. Brudvig, R. H. Crabtree, *Coord. Chem. Rev.* **1995**, *144*, 1. – [4d] V. L. Pecoraro, J. M. Baldwin, A. Gelasco, *Chem. Rev.* **1994**, *94*, 807. – [4e] R. Hage, *Recl. Trav. Chim. Pays-Bas* **1996**, *115*, 385. – [4f] K. Wieghardt, *Angew. Chem. Int. Ed. Engl.* **1989**, *28*, 1153; *Angew. Chem.* **1989**, *28*, 1153.
- [5] [5a] K. Kalyanasundaram, *Photochemistry of Polypyridine and Porphyrin Complexes*, Academic Press, London, **1992**. – [5b] V. Balzani, F. Scandola, *Supramolecular Photochemistry*, Ellis Horwood, Chichester, UK, **1991**. – [5c] H. Kurreck, M. Huber, *Angew. Chem. Int. Ed. Engl.* **1995**, *34*, 849. – [5d] M. R. Wasieleski, *Chem. Rev.* **1992**, *92*, 435. – [5e] V. Balzani, A. Juris, M. Venturi, S. Campagna, S. Serroni, *Chem. Rev.* **1996**, *96*, 759. – [5f] A. Osuka, S. Nakajima, T. Okada, S. Taniguchi, K. Nozaki, T. Ohno, I. Yamazaki, Y. Nishimura, N. Mataga, *Angew. Chem. Int. Ed. Engl.* **1996**, *35*, 92. – [5g] A. Harriman, J.-P. Sauvage, *Chem. Soc. Rev.* **1996**, *41*. – [5h] G. Steinberg-Yfrach, J.-L. Rigaud, E. N. Durantini, A. L. Moore, D. Gust, T. A. Moore, *Nature* **1998**, *385*, 239. – [5i] C. A. Slate, D. R. Striplin, J. A. Moss, P. Chen, B. W. Erickson, T. J. Meyer, *J. Am. Chem. Soc.* **1998**, *120*, 4885.
- [6] [6a] L. Sun, H. Berglund, R. Davydov, T. Norrby, L. Hammarström, P. Korall, A. Börje, C. Philouze, K. Berg, A. Tran, M. Andersson, G. Stenhagen, J. Mårtensson, M. Almgren, S. Styring, B. Åkermark, *J. Am. Chem. Soc.* **1997**, *119*, 6996. – [6b] L. Sun, L. Hammarström, T. Norrby, H. Berglund, R. Davydov, M. Andersson, A. Börje, P. Korall, C. Philouze, M. Almgren, S. Styring, B. Åkermark, *Chem. Commun.* **1997**, 607. – [6c] H. Berglund-Baudin, L. Sun, R. Davydov, M. Sundahl, S. Styring, B. Åkermark, M. Almgren, L. Hammarström, *J. Phys. Chem. A* **1997**, *102*, 2512.
- [7] G. Anderegg, E. Hubmann, N. G. Podder, F. Wenk, *Helv. Chim. Acta* **1977**, *60*, 123.
- [8] [8a] D. K. Towle, C. A. Botsford, D. J. Hodgson, *Inorg. Chim. Acta* **1988**, *141*, 167. – [8b] A. R. Oki, J. Glerup, D. J. Hodgson, *Inorg. Chem.* **1990**, *29*, 2435. – [8c] P. A. Goodson, A. R. Oki, J. Glerup, D. J. Hodgson, *J. Am. Chem. Soc.* **1990**, *112*, 6248.
- [9] [9a] J. A. Treadway, B. Loeb, R. Lopez, P. A. Anderson, F. R. Keene, T. J. Meyer, *Inorg. Chem.* **1996**, *35*, 2242. – [9b] L. Hammarström, F. Barigelletti, L. Flamigni, M. T. Indelli, N. Armadori, G. Calogero, M. Guardigli, A. Sour, J.-P. Collin, J.-P. Sauvage, *J. Phys. Chem. A* **1997**, *101*, 9061. – [9c] N. H. Damrauer, T. R. Bousie, M. Devenney, J. K. McCusker, *J. Am. Chem. Soc.* **1997**, *119*, 8253.
- [10] [10a] P. Finckh, H. Heitele, M. E. Michel-Beyerle, *J. Phys. Chem.* **1988**, *92*, 6584 and references therein. – [10b] A. Helms, D. Heiler, G. McLendon, *J. Am. Chem. Soc.* **1992**, *114*, 6227.
- [11] A. Magnuson, H. Berglund, P. Korall, L. Hammarström, B. Åkermark, S. Styring, L. Sun, *J. Am. Chem. Soc.* **1997**, *119*, 10720.
- [12] [12a] D. Burdinski, K. Wieghardt, S. Steenken, *J. Am. Chem. Soc.* **1999**, *121*, 10781. – [12b] D. Burdinski, E. Bothe, K. Wieghardt, *Inorg. Chem.* **2000**, *39*, 105. – [12c] L. Sun, M. K. Raymond, A. Magnuson, D. LeGourierrec, M. Tamm, M. Abrahamsson, P. Huang-Kenéz, J. Mårtensson, G. Stenhagen, L. Hammarström, S. Styring, B. Åkermark, *J. Inorg. Biochem.* **2000**, *78*, 15.
- [13] N. E. Tokel-Takvoryan, R. E. Hemingway, A. J. Bard, *J. Am. Chem. Soc.* **1973**, *95*, 6582.
- [14] P. Baekström, K. Stridh, L. Li, T. Norin, *Acta Chem. Scand.* **1987**, *B41*, 442.
- [15] L. Geren, H. Seung, B. Durham, F. Millett, *Biochemistry* **1991**, *30*, 9450.
- [16] S. Larsen, K. Michelsen, E. Pedersen, *Acta Chem. Scand.* **1986**, *A40*, 63.
- [17] A. Baba, W. Wang, K. W. Yong, L. Strong, R. H. Schmehl, *Synth. Comm.* **1994**, *24*, 1029–1036.
- [18] F. Krohnke, K. F. Gross, *Chem. Ber.* **1959**, *92*, 22.
- [19] T. J. Meyer, D. J. Salmon, B. P. Sullivan, *Inorg. Chem.* **1978**, *17*, 3334.
- [20] T. Urbanski, *J. Chem. Soc.* **1946**, 110.

Received April 17, 2000
[I00151]